Supplementary information for

Nanoconfinement of Microvilli Alters Gene Expression and Boosts T cell Activation

Morteza Aramesh [1, *], Diana Stoycheva [1], Ioana Sandu [2], Stephan J. Ihle [3], Tamara Zünd [1], Jau-Ye Shiu [1,4], Csaba Forró [5,6], Mohammad Asghari [7], Margherita Bernero [1], Sebastian Lickert [1], Annette Oxenius [2], Viola Vogel [1] and Enrico Klotzsch [1,8,*]

[1] Laboratory of Applied Mechanobiology, Department for Health Sciences and Technology, ETH Zürich, Zürich, Switzerland

[2] Institute of Microbiology, Department of Biology, ETH Zürich, Zürich, Switzerland

[3] Laboratory of Biosensors and Bioelectronics, Institute for Biomedical Engineering, ETH Zürich, Zürich, Switzerland

[4] Graduate Institute of Biomedical Sciences, China Medical University, Taichung 40402, Taiwan

[5] Department of Chemistry, Stanford University, Stanford, USA

[6] Tissue Electronics, Fondazione Istituto Italiano di Tecnologia, Largo Barsanti e Matteucci, 53-80125 Naples, Italy

[7] Institute for Chemical and Bioengineering, Department of Chemistry and Applied Biosciences, ETH Zürich, Zürich, Switzerland

[8] Institute for Biology, Experimental Biophysics/Mechanobiology, Humboldt University of Berlin, Berlin, Germany

Corresponding authors:

Morteza Aramesh, e-mail: morteza.aramesh@hest.ethz.ch

and Enrico Klotzsch, e-mail: enrico.klotzsch@hest.ethz.ch

Index

Other supplementary materials for this manuscript include the following:

Datasets S1: List of differentially expressed genes

Movie S1: 3D projection of actin protrusions of a jurkat cell into 200 nm pores of AAO membranes. Actin and nucleus were stained with Phalloidin and DAPI, and are shown in green and blue colors, respectively. Scale bar is 5 μm.

Movie S2: Live cell imaging of actin protrusions of a jurkat cell upon contact with a AAO membrane with 200 nm pores. Scale bar is 5 μm. Jurkat T cells were transfected with Lifeact-GFP.

Movie S3: Live cell imaging of actin protrusions of a jurkat cell on an AAO membrane with 200 nm pores. Scale bar is 5 μm. Jurkat T cells were transfected with Lifeact-GFP.

Movie S4: (Left) Live cell imaging of actin protrusions in a migrating jurkat cell on top of a AAO membrane with 200 nm pores. Scale bar is 5 μm. (right) a zoomed section from the trailing edge of the same cell on the left. Jurkat T cells were transfected with Lifeact-GFP.

Movie S5: Live cell imaging of cells on non-coated AAO with 200 nm pores. A jurkat cell retracts from the surface. Scale bar is 5 μm. Jurkat T cells were transfected with Lifeact-GFP.

Movie S6: Live cell imaging of cells on non-coated AAO with 200 nm pores. Actin treadmilling in a jurkat cell. Scale bar is 5 μm. Jurkat T cells were transfected with Lifeact-GFP.

1- Experimental

Materials:

Porous anodic aluminum oxide (AAO) are fabricated by anodization (electrochemical oxidation) of aluminum films, which results in formation of quasi-hexagonal arrays of nanopores with narrow distribution of pore size and interpore distances.[1,2]. The pore size and the distance between the pores, as well as the thickness, can be finely controlled by anodizing conditions such as voltage or electrolyte concentration. Pore sizes ranging from 20 to 450 nm can be obtained using this technique. [3] Furthermore, the surface of the oxide material can be functionalized with different coatings (such as polymer grafting)[2], well-established chemical reactions (such as silanization and protein binding)[4]. Importantly, the obtained oxide film is highly transparent (with refractive index of 1.77) which is entirely compatible with a wide range of optical microscopy techniques. AAO is a ceramic with stiffness within a range of 250-450 GPa.

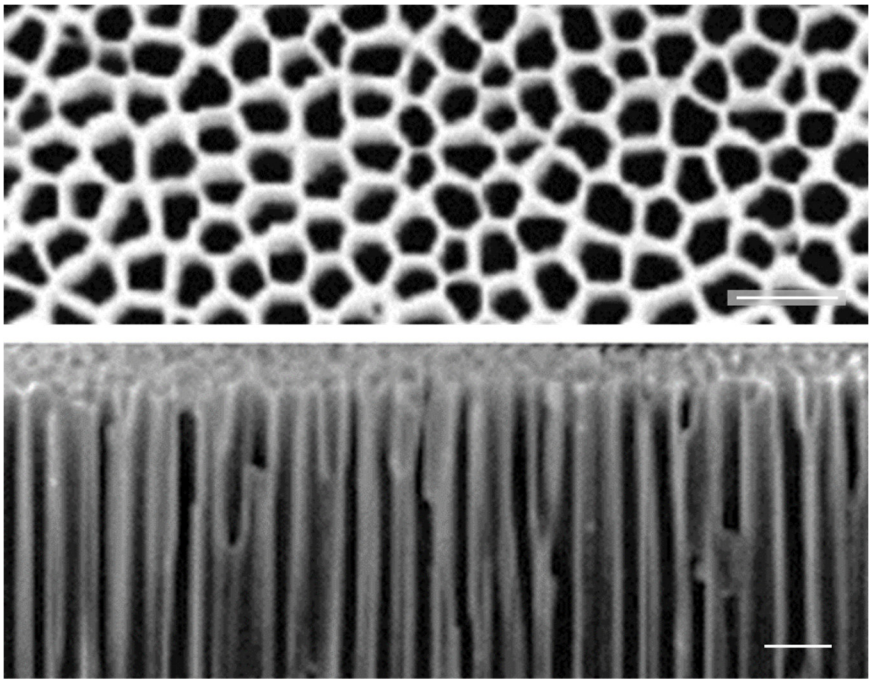

Figure S1. SEM images of ~200 nm pores in a porous AAO membrane. (top) shows the top view and (buttom) shows the cross-section view, scale bar is 500 nm.

Non-porous aluminum oxide samples were prepared by deposition of 40 nm of Al_2O_3 on a 13 mm round coverslip (1.5 H, 0117530, Marienfeld) using atomic layer deposition (ALD, Picosun Sunale R-150B). Briefly, ultrahigh-purity nitrogen carrier gas was purged at a flow rate of 200 sccm and a pressure of about 1 Torr was maintained. Al_2O_3 ALD was conducted with alternating exposures to trimethylaluminum (TMA) and water. TMA exposure and purge times were 0.1 and 4 s, respectively. The deposition was conducted at 150 °C with 400 cycles (0.1 nm/cycle).

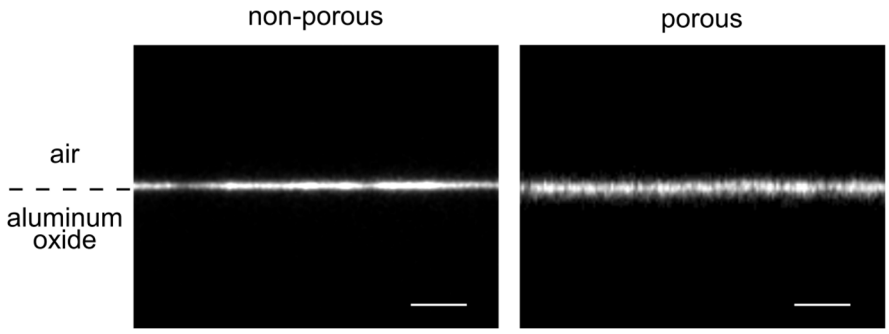

Figure S2. Streptavidin coated porous and non-porous samples. Z-stack images of the coated surface obtained by fluorescent microscopy. The samples were coated with streptavidin AlexaFluor 488, scale bar is 20 µm.

Isolation of the primary human T cells:

Pan T cells were purified from total peripheral blood from healthy adult volunteers. Freshly donated whole blood was first diluted to half with PBS (ROTI Cell PBS, Carl Roth) at room temperature. Then 35 mL of the diluted blood was added to 50 mL centrifuge tubes (SepMate, Stemcell Technologies) which were prefilled with 15 mL of density gradient medium (Lymphoprep, Stemcell Technologies). The samples were centrifuged at 1200 ×g for 10 min at room temperature. PBMCs in the top layer were washed with PBS and T cells were isolated by negative selection using EasySep Human Naïve Pan T cell Isolation Kit (Stemcell Technologies #17961), according to the manufacturer's protocol. Briefly, 50 µL of isolation cocktail antibodies and 50 µL of TCR gamma/delta depletion cocktail were added to 1 mL of Lymphoprep-purified PBMCs for 5 min at room temperature. Next, 60 µL of RapidSpheresTM were added per 1 mL of sample for another 3 min at room temperature, the sample was topped up to 2.5 mL and placed on a magnet (EasySep magnet, StemCell Technologies) for 3 min. The unlabeled cells were poured into a new tube, washed, counted and used for further applications.

High throughput RNA-Seq:

RNA extraction: Total RNA isolation was performed on stimulated and non-stimulated primary human T cells on porous and non-porous surfaces (porous± and non-porous±) after 4 hours of activation (3 samples and $5x10^5$ cells per condition). RNeasy Mini Kit (Qiagen) was used for RNA isolation. Briefly, 4h after activation, cells were collected in 1.5 mL eppendorf tubes and centrifuged for 5 min at 300 ×g to remove cell culture medium. Cell lysates were obtained by adding and vortexing the lysing buffer (350 µL per tube). The lysates were directly placed in the spin columns (QIAshredder) and were centrifuged at 8000 ×g for 2 min. 350 µL of 70% ethanol was added to the lysate and resuspended. RNeasy spin column was used to filter the RNA by centrifuging at 8000 ×g for 30 sec. RW1 buffer (700 µL) was used to wash the RNeasy column at 8000 ×g for 30 sec. Subsequently, 500 µL of RPE buffer was added to the RNeasy spin column and centrifuged at 8000 ×g for 30 sec. The washing step was repeated 3 times with the same conditions (2 times for 30 sec and 1 time for 2 min). The centrifugation was repeated without adding any buffer to reduce any possible carryover of the RPE buffer. To collect the RNA from the membrane, 50 µL of RNase-free water was added directly to the spin column and centrifuged for 1 min at 8000 ×g. The step was repeated by adding 37.5 µL of RNase-free water, and the flow-through was collected for DNase digestion before RNA clean up. DNase digestion was performed by adding 10 µL of RDD buffer and 2.5 µL of DNAse to 87.5 µL of RNA solution, and incubated for 30 min at room temperature. RNA cleanup procedure was performed by repeating the RNA isolation process, described above. In the final step, 50 µL RNase-free water was used to collect the RNA from the spin column membrane. RNA concentration and quality were determined by UV spectrophotometry (Nanodrop,Thermo Scientific). The ratio of absorbance at 260 nm and 280 nm was used to assess the purity of the extracted RNA. A ratio of >2.0 was accepted as a quality measure. The final concentration was 10-20 ng/µL. The samples were stored at -80 °C before sequencing.

RNA sequencing: High throughput RNA sequencing was performed by the technical staff of the Functional Genomics Center Zurich (FGCZ) of the ETH Zurich and the University of Zurich. Briefly, Illumina TruSeq mRNA

protocol was used for library preparation and sequencing was performed in an Illumina NovaSeq6000 (200 Million reads and 100 cycles).

Differential expression analysis: Differential expression analysis was conducted in R 3.6 [5]. All genes with fewer than 10 counts were removed. The filtered data was used for differential analysis ($log_2FC > 0.5$, adjusted p value < 0.05) with edgeR [6,7]. The p-values were adjusted for multiple comparisons with Benjamini-Hochberg method.

Plots: 2D multidimensional scaling plot of filtered data was generated with edgeR. Heatmaps were generated based on logged counts of the filtered data. For representations, the logged counts were scaled per gene and used to compute heatmaps with pheatmap package version 1.0.12 [8]. Volcano plots were generated with the EnhancedVolcano package [9] .

Gene-set enrichment analysis: For gene-set enrichment analysis, genes were ranked according to fold change between two groups of interest and analysis was performed with the fgsea package [10] in R. List of genes for the enrichment analysis were downloaded from MSigDB [11,12]. GO-term enrichment for a selected set of genes was performed with clusterProfiler [13] in R.

RT-qPCR:

Gene	Forward primer	Reverse primer
CD69	TCCAGGCCAATACACATTCTC	AGTCCAACCCAGTGTTCCTC
NFKB1	CAGGTCCAGGGTATAGCTTC	TGACCTCACCATTCCCAACG
TCR (TCRA)	CAGCTGAGAGACTCTAAATCC	AGTCAGATTTGTTGCTCCAGG
CD45 (PTPRC)	TGGAGGACACAGCACATTGG	GAGCAGCAATCATCACTTCAG
LFA-1 (ITGAL)	GAAGTGAGAGCAGGCTATTTG	CATGGATTGTCTGGACCTGG

Table S1: Primer sequences used for the amplification of target gene mRNAs.

Flow cytometry:

For surface staining cells were incubated with the following antibodies for 30 min at 4 °C: PerCP/Cy5.5 anti-human CD69 (clone FN50, BioLegend), APC anti-human CD25 (clone BC96, BioLegend), CD8 (clone SK1, BioLegend,), CD4 (clone OKT4, Biolegend), Alexa Fluor 647 anti-human TCR α/β (306714, BioLegend), Alexa Fluor 488 anti-human CD45 Antibody (368535, Biolegend). Proliferation was measured by dilution of CellTrace Violet (CTV Cell Proliferation Kit, Thermo Fisher Scientific, C34557) according to manufacturer's instructions. Shortly, cells were incubated with 5 µM CTV in PBS for 10 min at 37 °C and then washed with RPMI 1640 medium. Intracellular staining of phosphorylated ERK and pY20 were performed by fixing cells using 2% paraformaldehyde (Formaldehyde, 16%, methanol free, Ultra Pure, Polysciences, Inc) for 10 min at room temperature, and permeabilized with 100% ice-cold methanol on ice dropwise while vortexing. pERK was stained for 30 min using Alexa Fluor 647 anti-ERK1/2 Phospho Thr202/Tyr204 in PBS 1% bovine serum albumin BSA (clone 4B11B69, BioLegend). Phosphotyrosine was stained with pY20 antibody conjugated with Alexa Fluor 488 (BioLegend, 309306) in PBS 1% bovine serum albumin BSA for 30 min. Samples were acquired using LSRFortessa or FACSCanto II cytometers, or Diva Software (BD Biosciences, Allschwil, Switzerland), or CytoFLEX Flow Cytometer with CytExpert Software (Beckman Coulter, Inc.), depending on the availability. Data analysis was carried out using Flowjo v10.4.2 software (Treestar) as well as using Python 3 and the Cytoflow package.

ELISA:

Supernatants of cultured cells were obtained 24 hours after exposure of the cells to the surfaces. For Interleukin-2, Human IL-2 ELISA Set (Abcam, ab48471) was used according to the manufacturer's instructions. Supernatants were assessed in triplicates and at 1:4 and 1:5 dilutions. High-binding ELISA 96-well plates (Nunc, Thermo-Scientific) were coated with the coating buffer overnight at 4 °C. Plates were washed three times with the wash buffer (0.05% Tween-20 in PBS) and were blocked with 200 µL of 2% BSA in PBS for 2 h at room temperature. 100 µL of diluted supernatants and standards were added to the plates followed by addition of 50 µL of biotinylated

detection antibody and incubated for 1 h at room temperature. The plates were washed three times with the wash buffer, and 100 µL of diluted streptavidin-HRP was added and incubated for 30 min at room temperature. The plates were washed 3 times with PBS. 100 µL of TMB Substrate Solution was added into the wells and incubated in the dark for 10 minutes at room temperature. 100 µL of 1 M sulfuric acid (Sigma-Aldrich) was added to the wells to stop the reaction. A spectrometer (Tecan M200 Plate Reader) was used to read the absorbance of each well at 450 nm wavelength. The absolute concentration of IL2 in each well was calculated by mapping back to the standards (0-1000 pg/mL) using OriginLab 2019.

Immunostaining:

Cells were seeded on the surfaces (porous and non-porous, 50,000 cells per sample) and incubated at 37 °C and 5% CO_2 for the planned duration. All the buffers were pre-warmed at 37 °C. Then the cells were pre-fixed for 1 min in 0.5% PFA (Formaldehyde, Polysciences, Inc) in Cytoskeletal buffer (10 mM MES pH 6.1, 150 mM NaCl, 5 mM EGTA, 5 mM glucose, 5 mM $MgCl_2$). The cells were subsequently fixed and permeabilized with 4% PFA and 0.1% Triton-X in the Cytoskeletal buffer for 7 min. The samples were washed with PBS three times and incubated with 0.01% $NaCl_4$ in PBS for 10 min to reduce the autofluorescence. The samples were then washed with PBS for three times and were blocked with 2% BSA in PBS for 1 h at room temperature before staining. For staining TCR, pZAP70 and CD45 no pre-fixation step was implemented. The following reagents were used according to the manufacturers protocols for 1 hour at room temperature and dark: Phalloidin (Alexa Fluor 488, 546, 647 from Thermo Fisher Scientific) in 1:200 dilution, DAPI (4',6-Diamidino-2-Phenylindole, Dihydrochloride, Invitrogen) in 5 µg/mL concentration, anti-CD45 antibody (F10-89-4, Abcam and EP322Y, Abcam), anti-CD3 antibody (clone SP7, Abcam), anti-CD3 zeta phospho Y83 Alexa Fluor 647 (clone EP776(2)Y, Abcam), Anti-alpha Tubulin antibody, Microtubule Marker (ab15246, Abcam), TCR alpha/beta Monoclonal Antibody (clone IP26, 14-9986-82, Thermo Fisher Scientific), Phospho-Zap-70 Tyr319 (clone 65E4, Cell Signaling Technology), Vybrant DiD Cell-Labeling Solution (Invitrogen, V-22887). 1% BSA in PBS was used as a buffer to dilute the antibodies. The secondary antibodies were added (for samples with unconjugated antibodies). The secondary antibodies were added (for samples with unconjugated antibodies) and incubated 2 hours at room temperature in the dark. The samples were then washed with PBS three times (1, 1 and 10 min at room temperature in the dark) before mounting with Prolong gold antifade reagent (Molecular Probes).

ERK Inhibition:

ERK inhibition was achieved by incubating cells with U0126 (Abcam, ab120241) at different doses (0, 0.1, 1 and 10 µM diluted in Anhydrous DMSO (Sigma-Aldrich). The cells were then incubated with the porous/non-porous surfaces for 0-60 min and 24 hours. The cell concentration was 5×10^5 cells/mL.

Polymer coating:

AAO membrane was first spin coated with photoresist (PR) AZ1518 (MicroChemicals GmbH) at 1750 rpm for 1 min and baked at 100 °C for 3 min. Reactive-ion etching (RIE) (Oxford, Plasmalab 80) was used to create and control different depths of nanohole on composite AAO-PR substrate. AAO-PR substrates were etched by RIE for 10, 15, 20 and 30 min with O_2: 20 sccm and RF power of 100 watt, achieving the respective depths of 0.5, 1, 2 and 4 µm. The AAO-PR nanohole was sputter coated with a 5 nm layer of Pt for SEM (Zeiss ULTRA 55) analysis.

Optical microscopy:

For all confocal Z-stack images SP8 confocal laser scanning microscope (Leica) was used to acquire images using 40× and 63× (1.4 NA Oil objective) objectives, and Leica LAS X SP8 Version 1.0 software.

For super-resolution images, 3D structured illumination microscopy (Deltavision OMX V4) was used. Diode lasers with 405 and 488 were used for illumination, with DAPI 420-451 and GFP 504-552 nm emission filters. The signals were recorded by the sCMOS OMX V4 (15bit range) detector. The objective was PlanApoN 60× with 1.42 NA and

oil immersed. The data was acquired with DeltaVision OMX (3.30.4378.0) software, and was reconstructed with softWoRx 6.0 (5.9.9) software. The nominal resolution of the microscope was 120-160 nm (lateral- xy) and 280-350 nm (axial-z). The cells were fixed after 30 min exposure to the surfaces, where actin was stained with Phalloidin Alexa Fluor 488 and the nucleus was stained with DAPI.

For live-cell imaging, an upright laser scanning confocal microscope (LSM 780, Zeiss AxioImager.Z2) was used with a water dipping lense (40×/0.75NA N-Achroplan M27) that allowed visualization of fluorescent signal from the top. Argon laser (with 0.1% power) and GFP filters (BP470/40 for excitation and BP525/50 for emission) were used for data acquisition. The system was equipped with a stage top incubator including temperature control and CO_2 (Pecon). Samples were placed in 6 well-plates, with 1.5 mL RPMI 1640 medium.

Electron microscopy:

For electron microscopy images, human primary T cells were exposed to the porous/non-porous surfaces for 30 min in 6 well-plates and subsequently fixed with GA (glutaraldehyde, Sigma-Aldrich, G7651-10X10ML). 50% GA stock solution was diluted to 2.5% in 0.1 M sodium cacodylate buffer (Electron Microscopy Sciences, 11654) and warmed to 37 °C. First, the cells were gently washed once with the pre-warmed 0.1 M sodium cacodylate buffer, which was immediately replaced with 2.5% GA and incubated for 20 min at room temperature. The samples were then washed with 0.1 M sodium cacodylate buffer three times. Another washing step was performed with PBS for three times, prior to the stepwise dehydration with ethanol by Pelco Biowave Microwave (TED PELLA), according to the manufacturer's protocol. The samples were transferred to a critical point dryer system (CPD 931, Tousimis) to remove the ethanol. 2 nm Pt was sputter coated on the samples (using CCU-010 Metal Sputter Coater, Safematic). High resolution scanning electron images were obtained by a field-emission gun SEM (FEI Quanta 200F), at 10 kV, high vacuum and working distance of 9 mm.

Statistical methods:

All statistical analyses were performed using R. All values are expressed as the mean ± s.d. The significance between the groups were measured using two-sided Mann-Whitney tests, unless otherwise noted.

2- Supplementary Figures

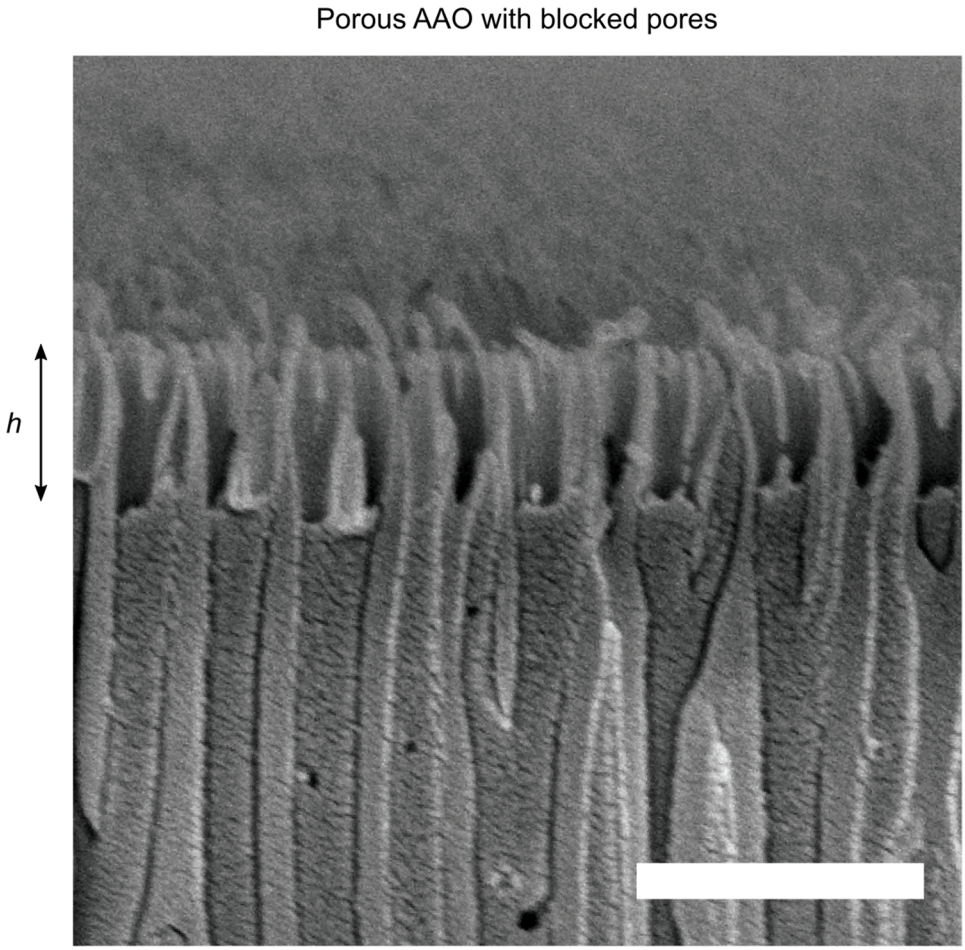

Figure S3-1. A SEM image of a porous AAO membrane that was filled with a polymer to the depth h. The example image shows the pores that were filled to the depth of h = 1 μm from the top surface. This was achieved by controlled RIE etching of the polymer (PR AZ1518, MicroChemicals GmbH) that was spin coated on the surface. Scale bar is 2 μm.

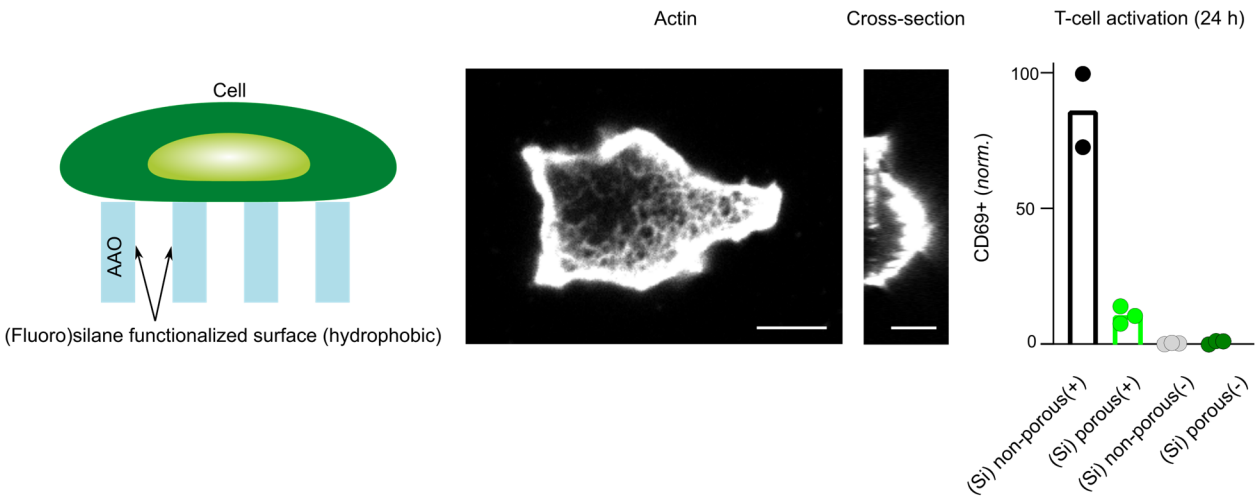

Figure S3-2. (left) Schematic shows silane modification of AAO surfaces using Trichloro(1H,1H,2H,2H-perfluorooctyl)silane, which results in strong hydrophobicity. (middle) The confocal images of actin structure in a representative cell show that the cells were only settled on the top surface and did not form protrusions into the pores of the silanized AAO samples. Scale bar is 5 µm. (right) Bar diagrams show activation of Jurkat T cells on silanized porous/non-porous surfaces. CD69 expression was measured after 24 hours. Data is a representation of two independent experiments performed in duplicates or triplicates. +/- signs indicate the presence of activation antibodies (αCD3/CD28) on the surface.

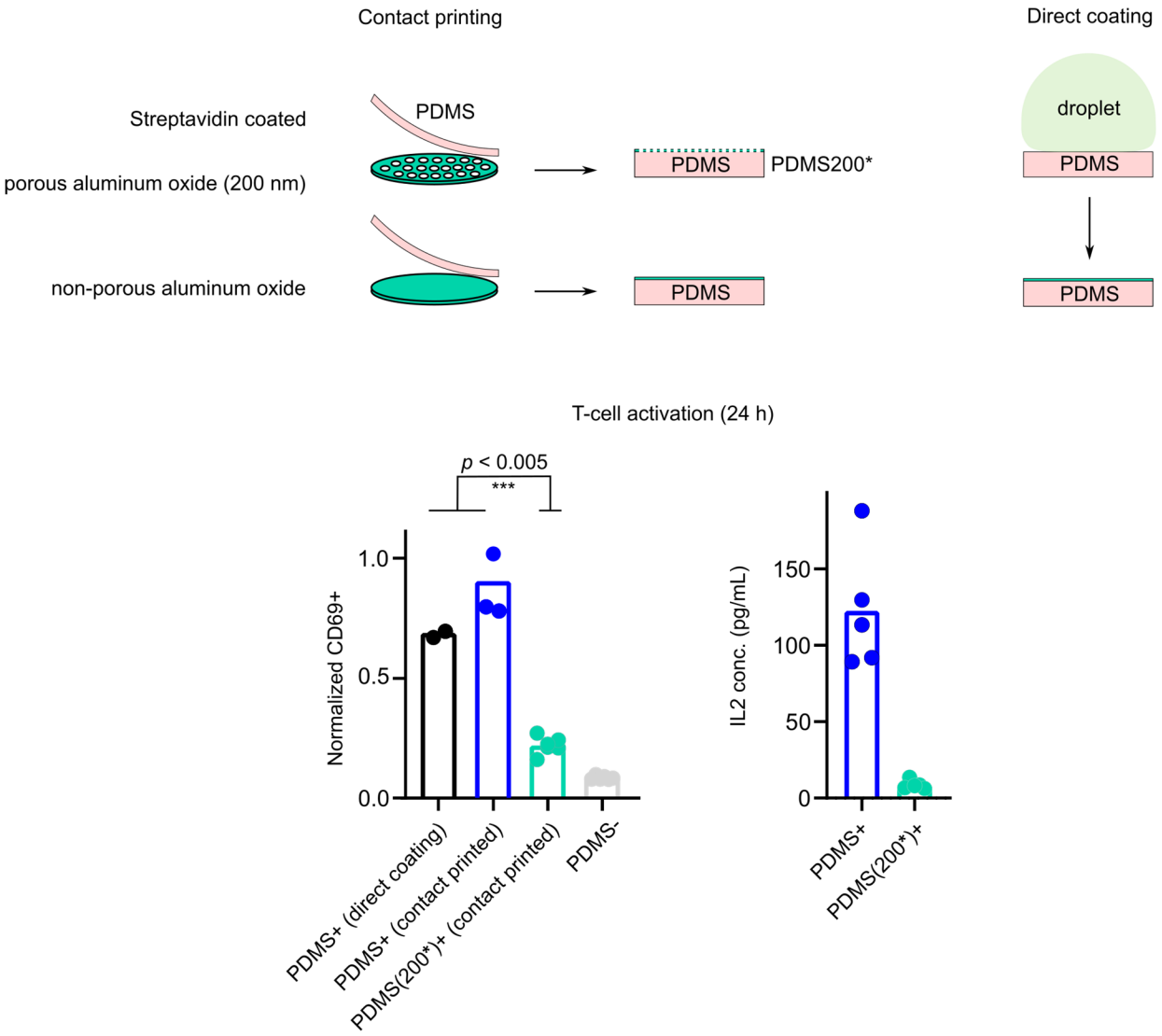

Figure S3-3. (top) 2D pattern transfer using micro(nano)-contact printing. Surfaces of porous/non-porous aluminum oxide films were coated with streptavidin. A PDMS was used to strip the streptavidin from the coated surfaces [14]. BSA was used to block nonspecific binding of biotin and streptavidin, before the addition of biotinylated antibodies. For comparison, a PDMS was coated with direct coating using a droplet of diluted streptavidin. (bottom) Bar diagrams show activation of Jurkat T cells on PDMS with/without nanopatterns, PDMS(200*)+ and PDMS+ (contact printed), respectively. A directly coated PDMS surface, PDMS+(direct coating), was used for comparison of the results. CD69 expression and IL2 secretion were measured after 24 hours. Two independent experiments were performed in duplicates and triplicates. + sign indicates the presence of activation antibodies (αCD3/CD28) on the surface.

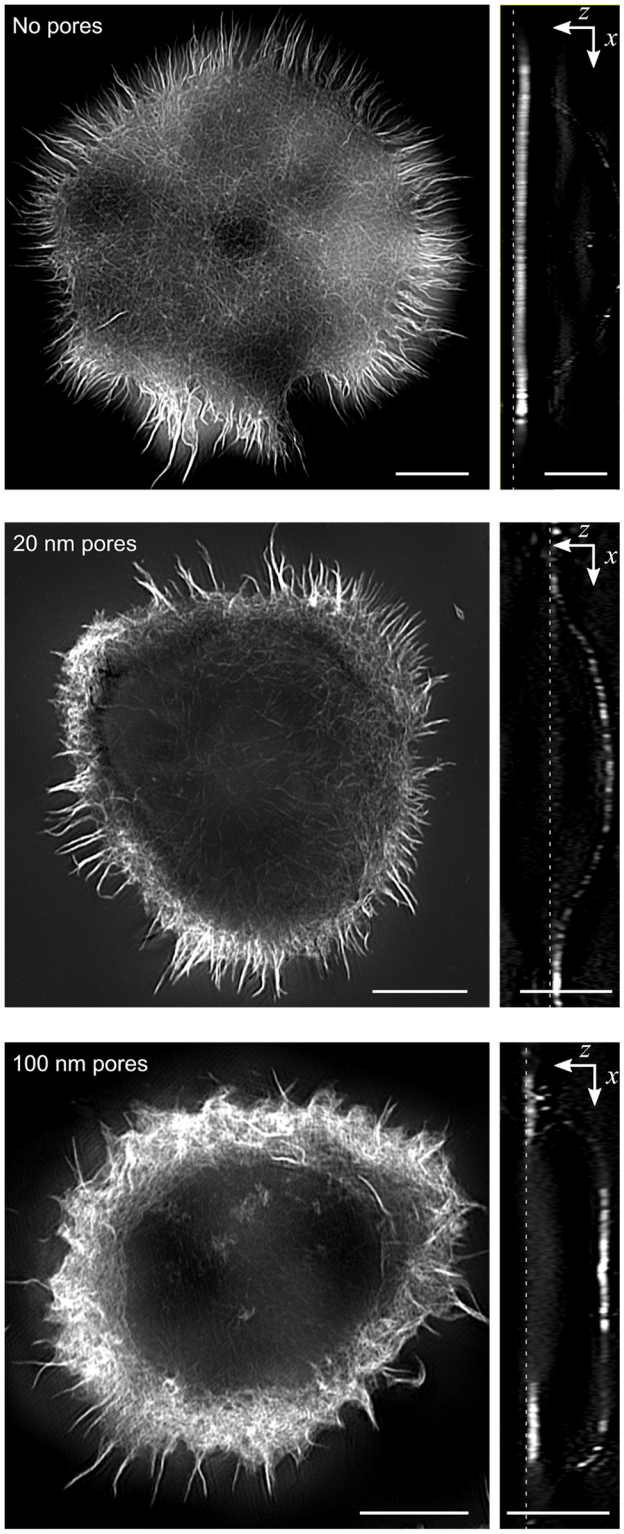

Figure S4-1. Super-resolution images of actin cytoskeleton in a T cell using structured illumination microscopy. Cells were placed on top of the flat or porous membranes with different pore sizes. No protrusions were detected on samples with pores < 200 nm in diameter. Scale bar 5 μm.

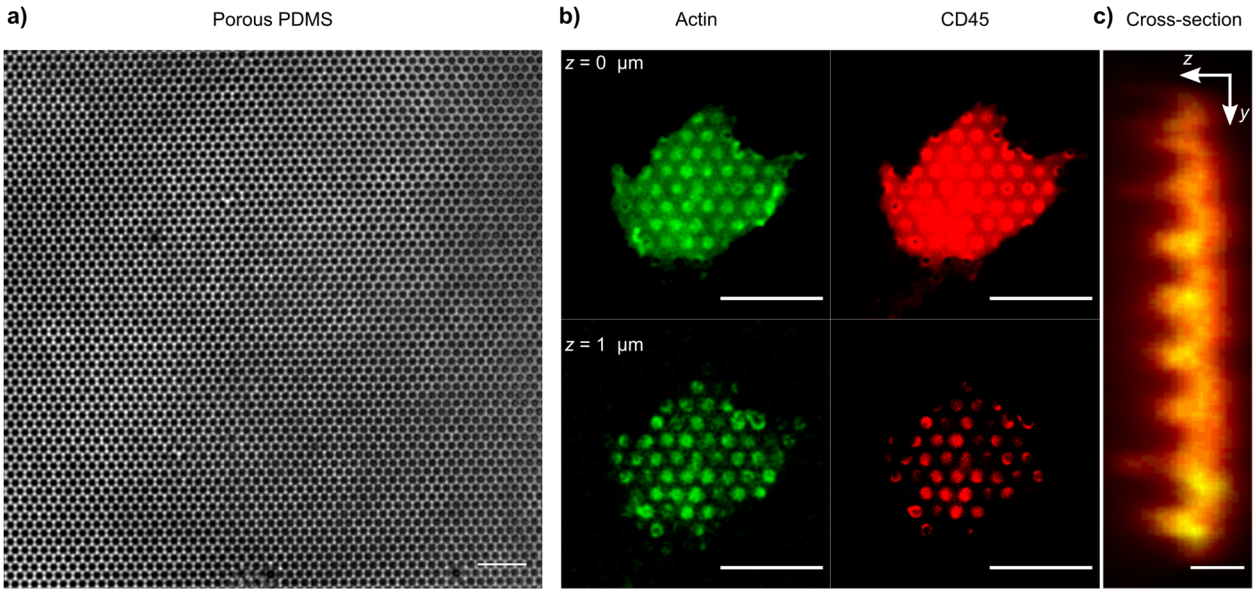

Figure S4-2. (a) Bright-field image of the porous PDMS, scale bar 10 µm. (b) Confocal fluorescent microscopy images of jurkat T cells on top of the porous PDMS (without αCD3/CD28 coatings), scale bar 10 µm. Cells were fixed and stained with actin and CD45, 30 min after the exposure to the surfaces. c) The cross-section view of the protrusions in PDMS micropores (1 µm), indicating the presence of actin and CD45 in the protrusions, scale bar 2 µm.

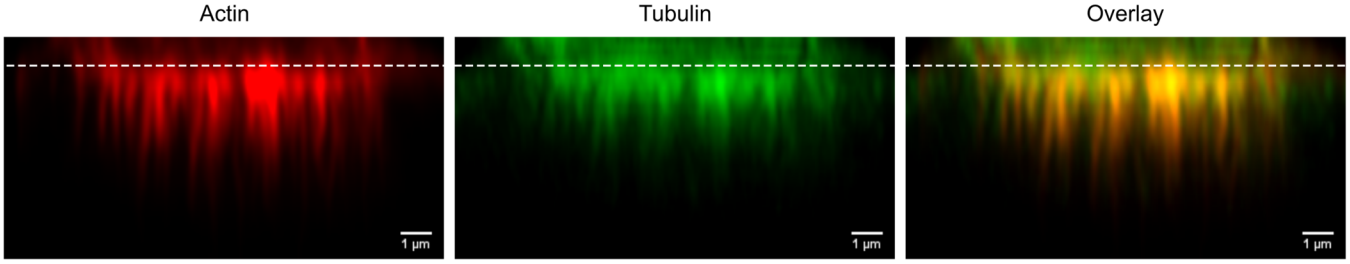

Figure S4-3. Microtubules inside of the 400 nm pores. A cross--section view of a Jurkat T cell on a porous AAO with 400 nm pore size, captured by Airyscan confocal microscopy. The cells were stained with phalloidin (actin cytoskeleton) and anti-tubulin (microtubules), indicating that the microtubules enter into the 400 nm pores, scale bar 1 µm.

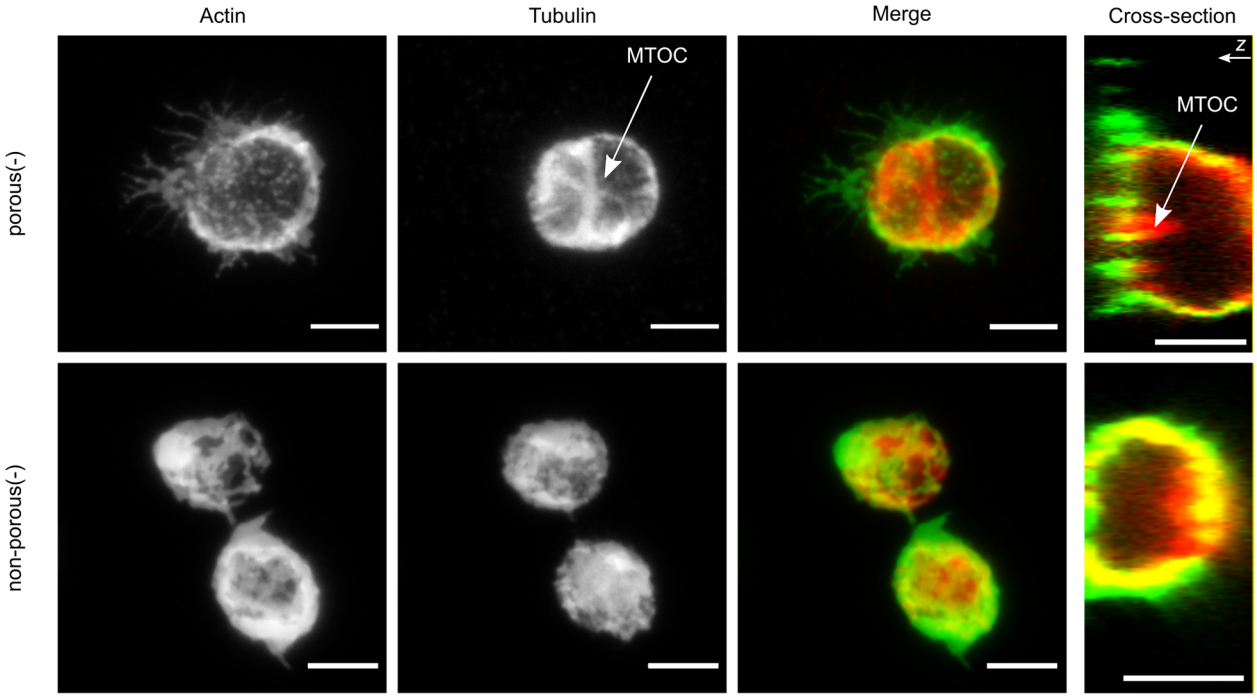

Figure S4-4. Confocal fluorescent microscopy images of primary human T cells on top of the 200 nm porous (-) and non-porous (-) surfaces (without αCD3/CD28 coatings), scale bar 5 μm. Cells were fixed and stained with actin and tubulin, 30 min after the exposure to the surfaces. Cells on porous surfaces are generally larger than the cells on non-porous surfaces. Actin protrusions appear as dotted structures on the porous surface. Moreover, the microtubule-organizing center (MTOC) is structured differently on the porous surface compared to the non-porous surface. MTOC translocation is known to be correlated with immunological synapse formation and sustained T cell signaling[15].

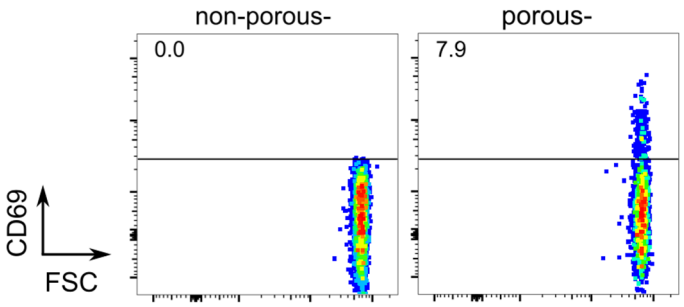

Figure S5-1. CD69 expression. The graphs represent examples of the measurements by flow cytometry 24 hours after primary human T cell activation/stimulation on porous (200 nm) and non-porous surfaces. - signs indicate the absence of activation antibodies (αCD3/CD28) on the surface.

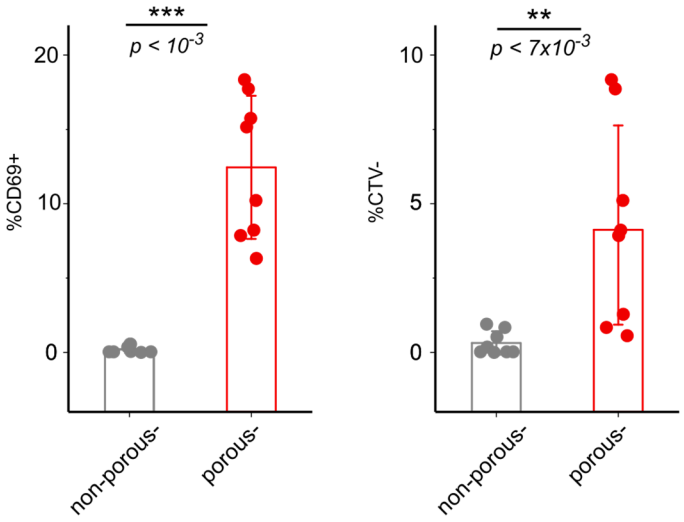

Figure S5-2. Bar diagrams show activation of primary human T cells on porous (200 nm) and non-porous surfaces. CD69 expression was measured after 24 hours of seeding the cells on the surfaces.Proliferation was measured 4 days after the seeding via a dye dilution assay (CTV). - sign indicates the absence of activation antibodies (αCD3/CD28) on the surface.

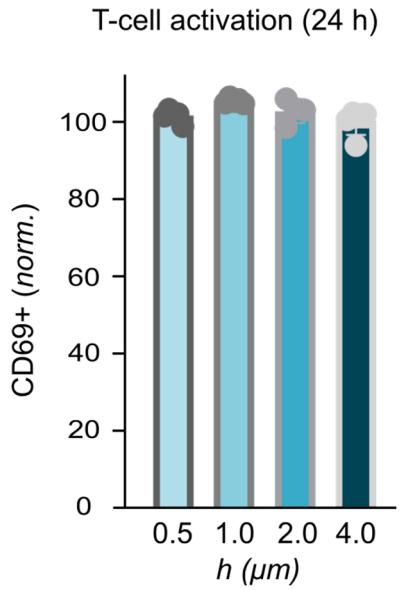

Figure S5-3. Bar diagrams show CD69 expression of activated Jurkat T cells on polymer coated porous AAO membranes (200 nm), to different depths. Data is a representation of two independent experiments (5 replicates). All the samples were coated with activation antibodies (αCD3/CD28).

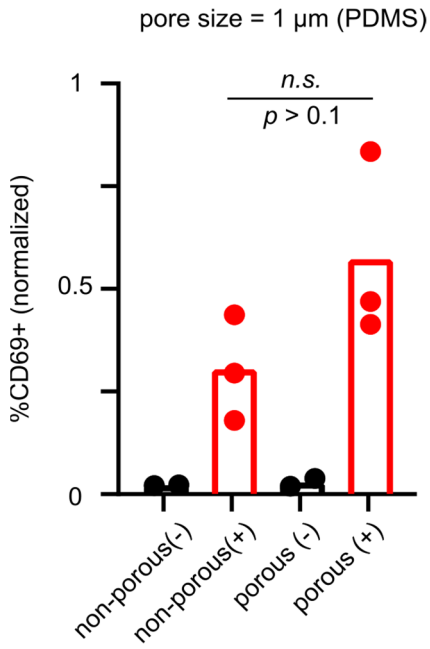

Figure S5-4. Bar diagrams show CD69 expression of activated Jurkat T cells on porous PDMS (with 1 μm pore size and 3 μm spacing) and non-porous PDMS surfaces (3 replicates). +/- signs indicate the presence of activation antibodies (αCD3/CD28) on the surface.

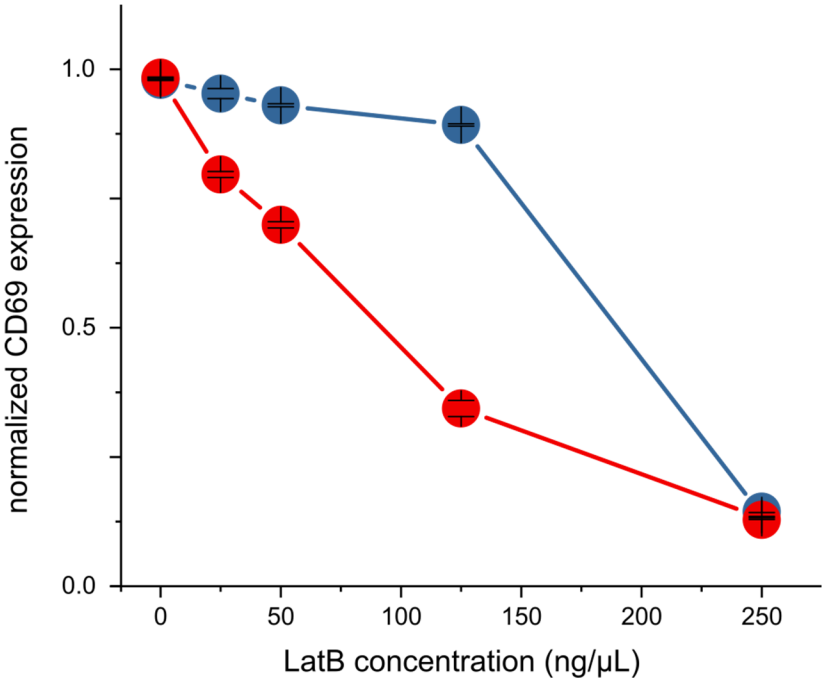

Figure S5-5. Normalized CD69 expression in activated Jurkat T cells on porous (red) and non-porous (blue) surfaces, after treatment with Lat B. Cells were incubated with Lat B at different concentrations for 30 min at 37 °C. The cells were washed with PBS and then seeded on the surfaces coated with activation antibodies (αCD3/CD28). CD69 expression was measured 24 hours after activation. The activation was reduced with Lat B concentration, where the changes on the porous surface (200 nm) was more sensitive to the drug compared to the flat surface. Note that F-actin polymerization is required for T cell activation, therefore by increasing Lat B concentration, activation efficiency decreases. This becomes more obvious at higher concentrations of Lat B (*e.g.* 250 ng/µL), where activation is fully impaired.

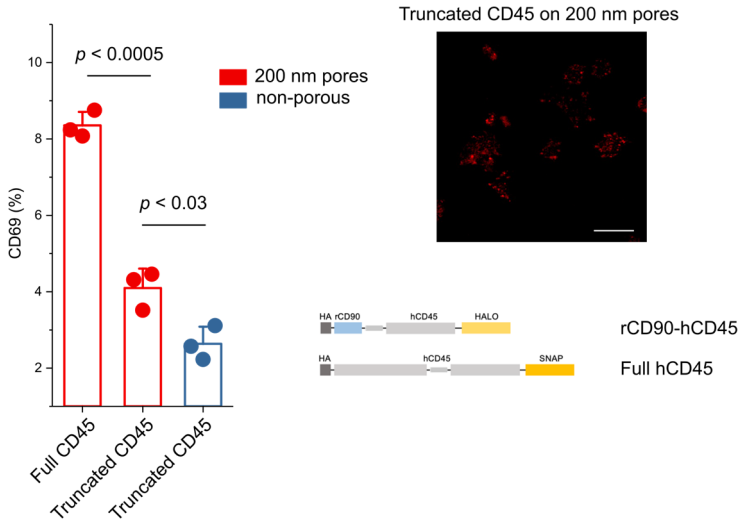

Figure S5-6. Bar diagrams show CD69 expression of Jurkat T cells with full and truncated CD45 on 200 nm pores and non-porous surfaces (3 replicates). The surfaces were not coated with activation antibodies (αCD3/CD28). Confocal fluorescent microscopy image shows the dotted structure (associated with the protrusions) of Jurkat T cells with truncated CD45 inside of the 200 nm pores.

Note: The cell lines used for these experiments were kind donations from Simon Davis lab. Briefly, the CD45 truncated cell line is a Jurkat cell line ("J8") that expresses a rCD90/CD45 chimera. The control (full CD45) is also a Jurkat cell line ("J8") and is a closely matched line that expresses full-length CD45. Please refer to Irles et al. [16]

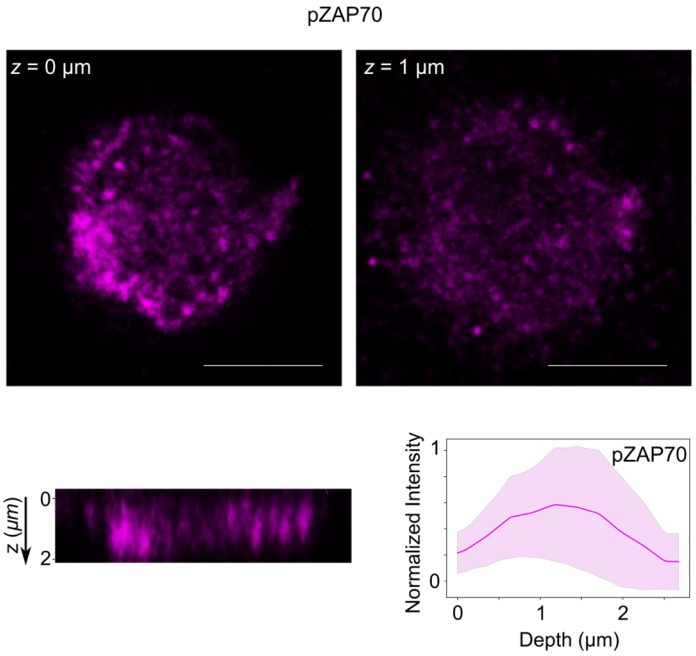

Figure S6-1. Confocal fluorescence microscopy images of phosphorylated ZAP70 (pZAP70), from T cells on a 200 nm porous surface at the basal membrane (upper left) or inside the pores (upper right). (bottom) shows the cross-section of the protrusions inside of the pores with the normalized intensity profile plotted on the right.

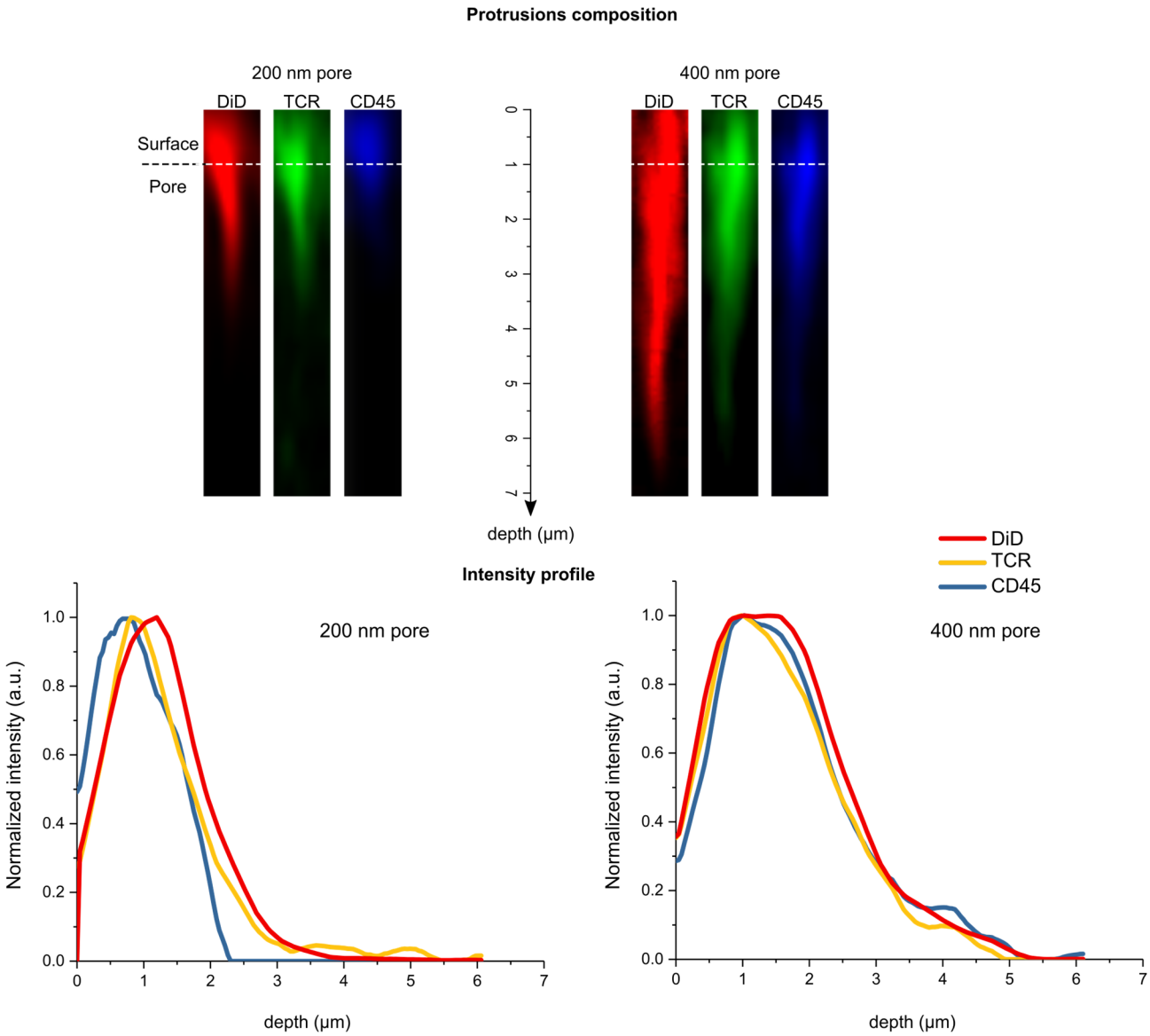

Figure S6-2. Cross-section of protrusions into the pores with 200 nm and 400 nm in diameter (n = 10). The membrane of the cells were stained with DiD, TCR and CD45. The intensity profile of the protrusions indicates spatiotemporal segregation of T cell receptors excluding CD45 phosphatases from the nanopore protrusions.

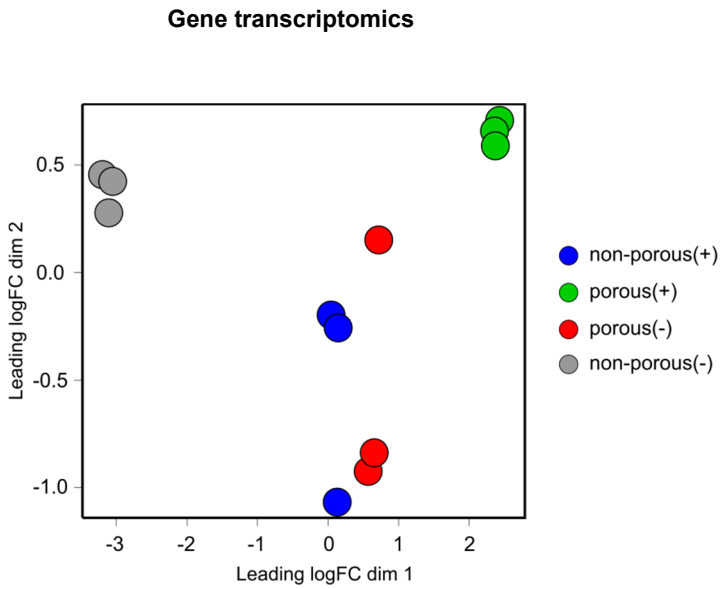

Figure S7-1. Multidimensional scaling (MDS) analysis of gene expression data of primary human T cells activated for 4 h on the indicated surfaces. The genes used for this analysis were filtered (more than 10 counts). Porous is 200 nm AAO, non-porous is aluminum oxide surface. +/- signs indicate the presence of activation antibodies (αCD3/CD28) on the surface.

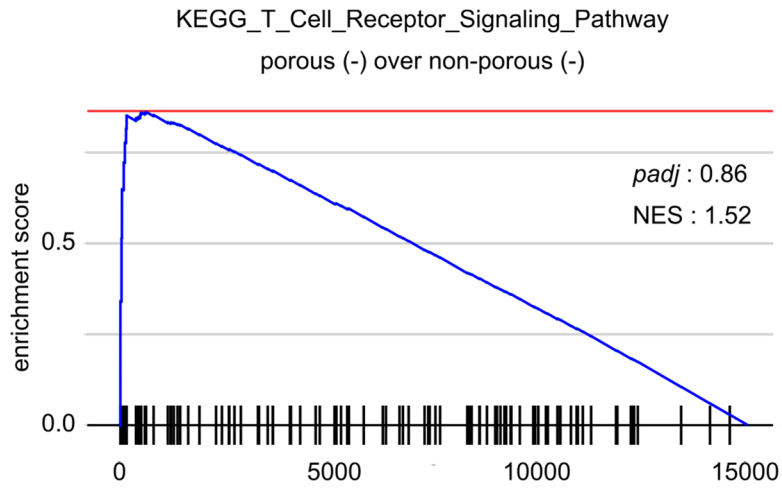

Figure S7-2. Gene set enrichment analysis of the TCR signaling pathway (KEGG) of porous(-) vs non-porous(-), without stimulating antibodies. - sign indicates the absence of activation antibodies (αCD3/CD28) on the surface. The ranking of genes was based on the fold change between the two specified groups. The leading genes were: "CSF2", "IL2", "TNF", "PDCD1", "FOS", "IFNG", "MAP3K8", "NFKB1", "IL10", "CTLA4", "NFKBIA", "CDK4", "CD40LG", "VAV3".

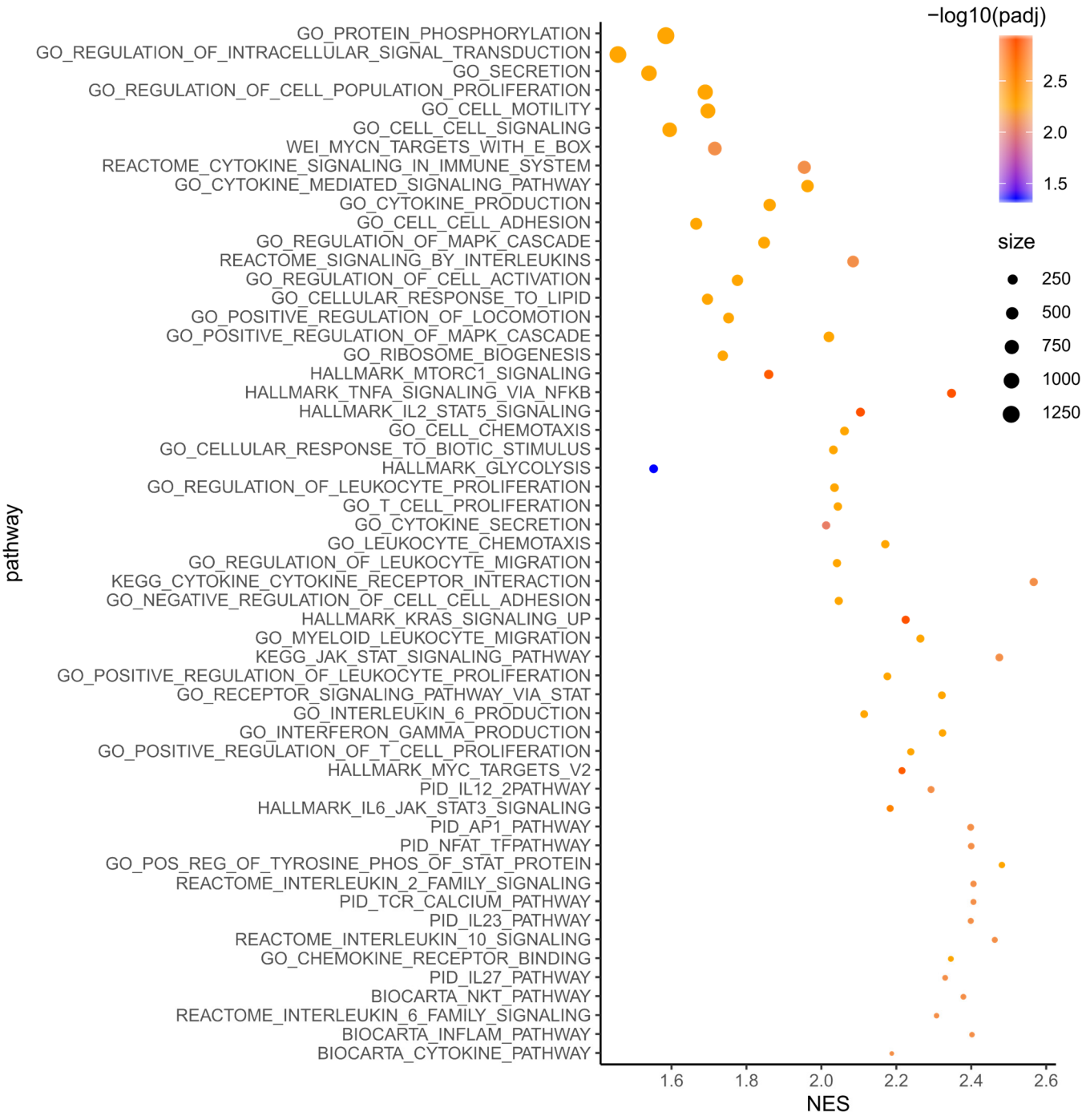

Figure S7-3. Pathway enrichment of differentially expressed genes in porous(+) cells versus non-porous(+). The size of the circle corresponds to the gene counts (from the reference pathway), the color corresponds to the adjusted P value. N.b. A selection of these pathways is represented in Figure 1e of the main manuscript.

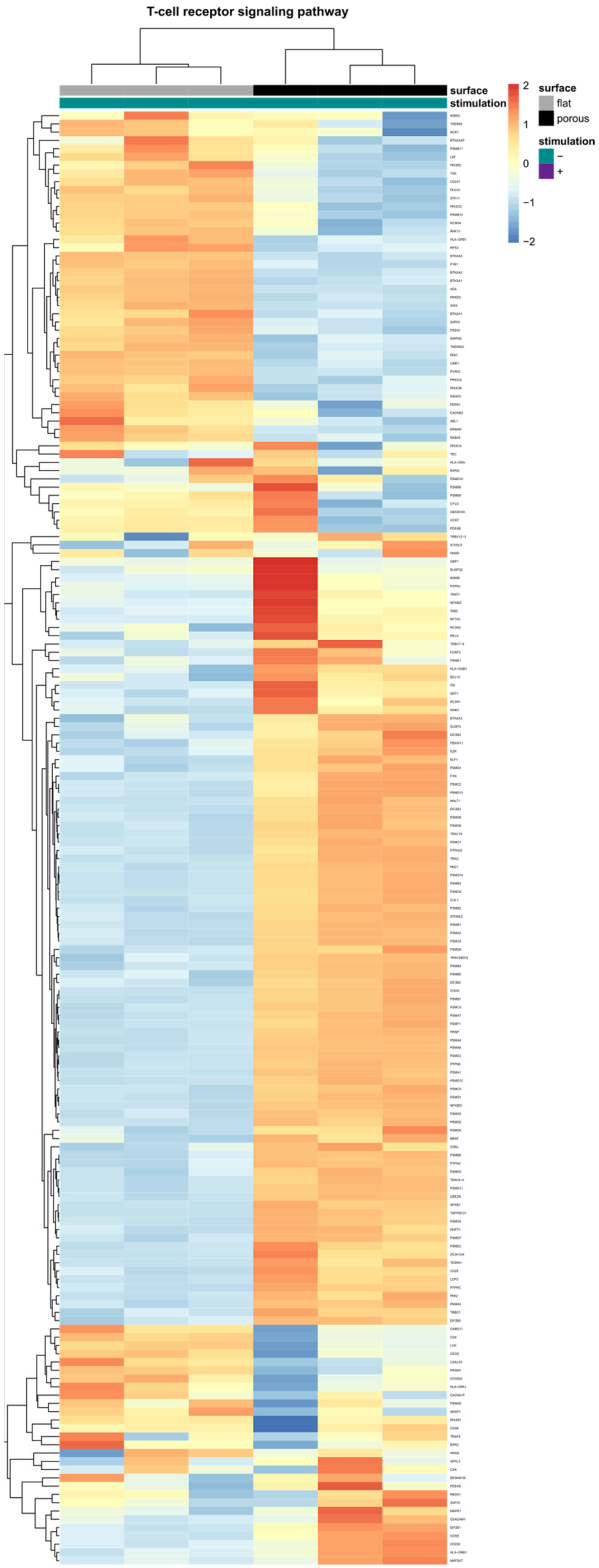

Figure S7-4. Heatmap of the all significantly upregulated or downregulated genes in theT cell receptor signaling pathway of primary human T cells on top of the porous (-) and non-porous (-) surfaces (without αCD3/CD28 coatings). Genes in the pathway of primary human T cells in porous(-) were compared to non-porous(-) (n = 3 replicates). The full list of the genes is provided in Dataset S1.

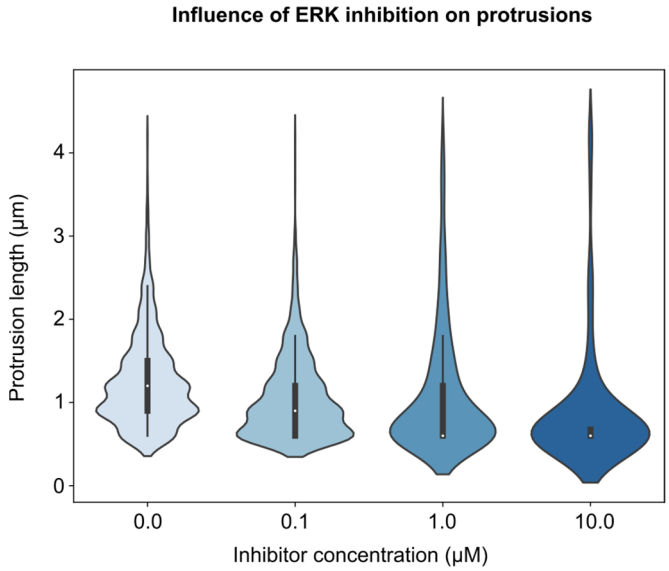

Figure S8-1. MAPK pathway was inhibited by incubating the cells with an inhibitor at different concentrations. The protrusions' length was measured on fixed cells after 30 min of activation. The Violin plot shows the distribution of the measured lengths (n = 20 cells). The bar histogram shows the average number of protrusions per cell vs protrusion lengths.

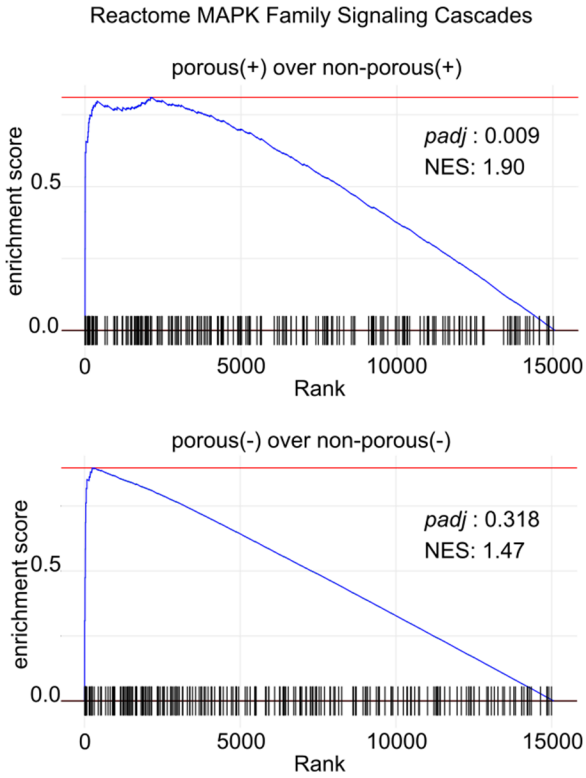

Figure S8-2. Gene set enrichment analysis of the MAPK family signaling cascade (Reactome). (top) is porous(+) vs non-porous(+). (bottom) is porous(-) vs non-porous(-). MAPK pathway is enriched on the porous surfaces, with/without stimulating antibodies. +/- signs indicate the presence of activation antibodies (αCD3/CD28) on the surface. The ranking of genes was based on the fold change between the two specified groups.

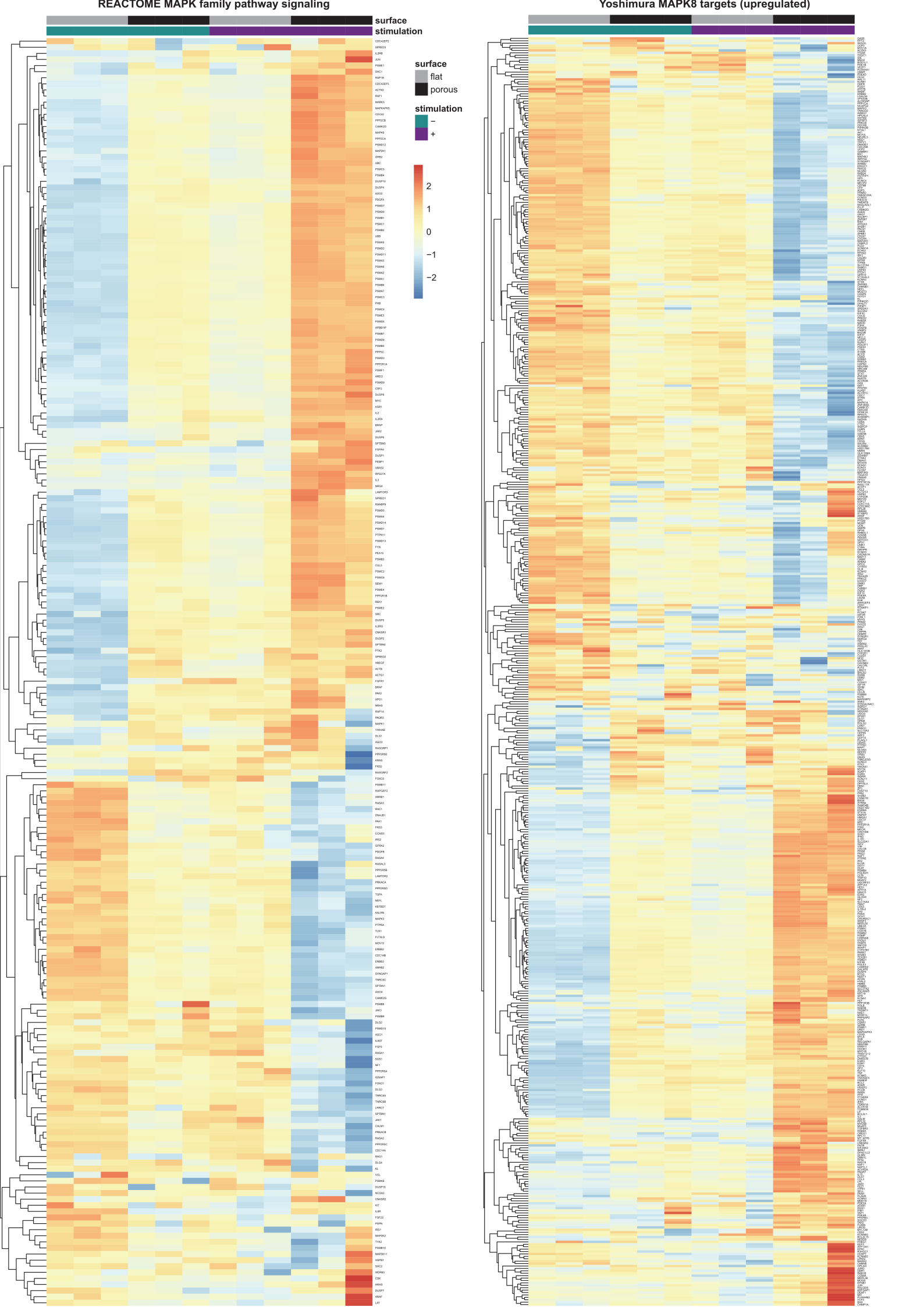
REACTOME MAPK family pathway signaling
Yoshimura MAPK8 targets (upregulated)
surface
stimulation
surface
flat
porous
stimulation
–
+
2
1
0
−1
−2

Figure S8-3. Heatmap of all significantly upregulated or downregulated genes in the MAP Kinase pathway of primary human T cells activated on the indicated surfaces for 4 h, adjusted P values < 0.05. Genes in porous(+) were compared to non-porous(-) cells (n = 3 replicates).

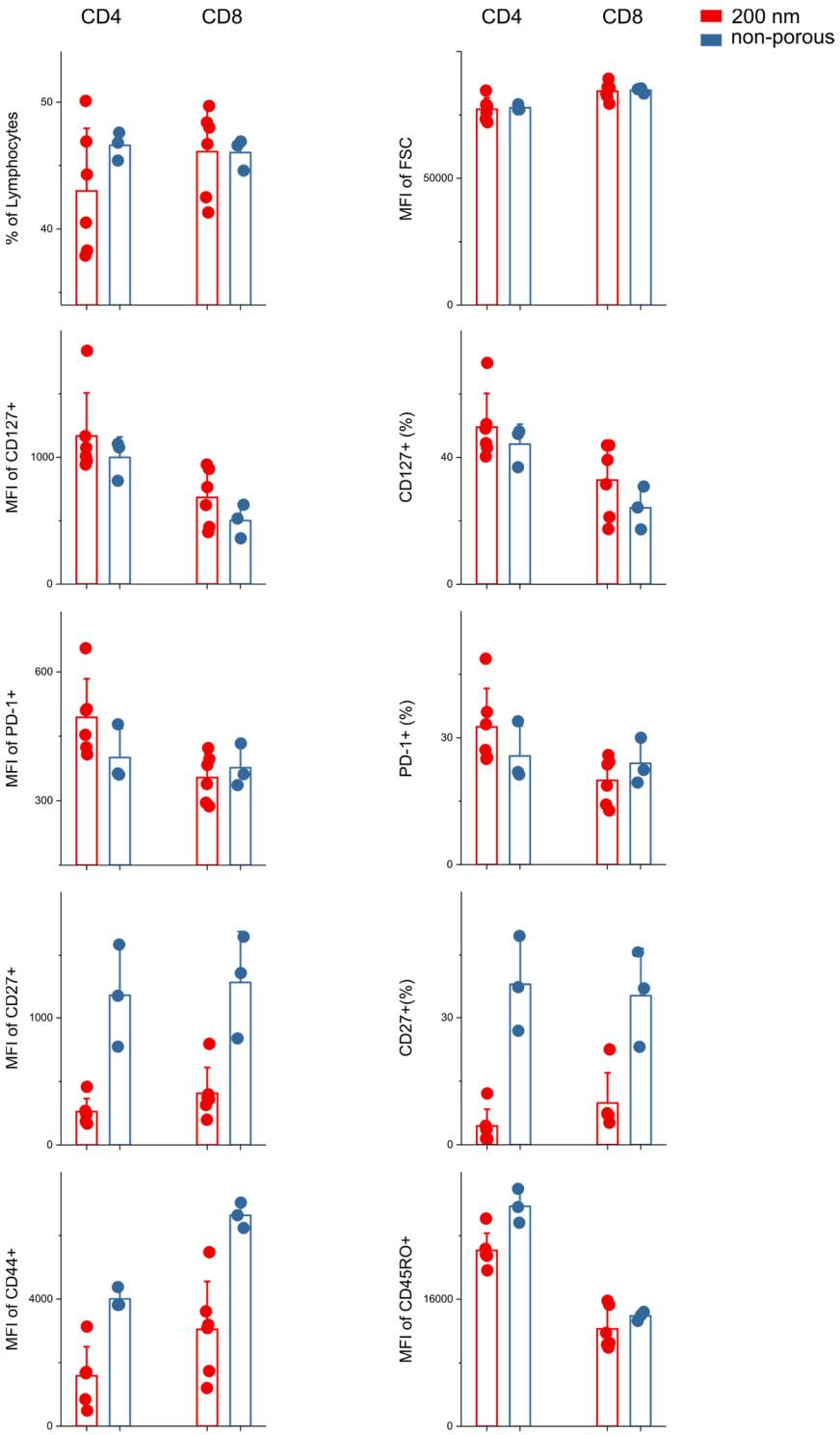

Figure S9. Phenotype analysis of activated T cells (day 8), using porous or non-porous surfaces.

3- Supplementary References

1. Lee, W. & Park, S.-J. Porous anodic aluminum oxide: anodization and templated synthesis of functional nanostructures. *Chem. Rev.* **114**, 7487–7556 (2014).
2. Aramesh, M. & Cervenka, J. Surface modification of porous anodic alumina for medical and biological applications. *pdfs.semanticscholar.org* (2014).
3. Nanoporous anodic aluminium oxide: Advances in surface engineering and emerging applications. *Prog. Mater Sci.* **58**, 636–704 (2013).
4. Yamaguchi, A. *et al.* Self-assembly of a silica–surfactant nanocomposite in a porous alumina membrane. *Nat. Mater.* **3**, 337–341 (2004).
5. R: The R Project for Statistical Computing. http://www.R-project.org/.
6. Robinson, M. D., McCarthy, D. J. & Smyth, G. K. edgeR: a Bioconductor package for differential expression analysis of digital gene expression data. *Bioinformatics* **26**, 139–140 (2010).
7. McCarthy, D. J., Chen, Y. & Smyth, G. K. Differential expression analysis of multifactor RNA-Seq experiments with respect to biological variation. *Nucleic Acids Res.* **40**, 4288–4297 (2012).
8. Kolde, R. pheatmap: Pretty Heatmaps. (2019).
9. Blighe, K., Rana, S. & Lewis, M. EnhancedVolcano: Publication-ready volcano plots with enhanced colouring and labeling. R package version 1.4.0. (2019).
10. Korotkevich, G., Sukhov, V. & Sergushichev, A. Fast gene set enrichment analysis. doi:10.1101/060012.
11. Subramanian, A. *et al.* Gene set enrichment analysis: a knowledge-based approach for interpreting genome-wide expression profiles. *Proc. Natl. Acad. Sci. U. S. A.* **102**, 15545–15550 (2005).
12. Liberzon, A. *et al.* The Molecular Signatures Database (MSigDB) hallmark gene set collection. *Cell Syst* **1**, 417–425 (2015).
13. Yu, G., Wang, L.-G., Han, Y. & He, Q.-Y. clusterProfiler: an R Package for Comparing Biological Themes Among Gene Clusters. *OMICS: A Journal of Integrative Biology* vol. 16 284–287 (2012).
14. Tiefenauer, R. F., Tybrandt, K., Aramesh, M. & Vörös, J. Fast and Versatile Multiscale Patterning by Combining Template-Stripping with Nanotransfer Printing. *ACS Nano* **12**, 2514–2520 (2018).
15. Martín-Cófreces, N. B. *et al.* MTOC translocation modulates IS formation and controls sustained T cell signaling. *J. Cell Biol.* **182**, 951–962 (2008).
16. Irles, C. *et al.* CD45 ectodomain controls interaction with GEMs and Lck activity for optimal TCR signaling. *Nat. Immunol.* **4**, 189–197 (2003).